Development/Plasticity/Repair

Requirement of Adenylate Cyclase 1 for the Ephrin-A5-Dependent Retraction of Exuberant Retinal Axons

Xavier Nicol, Aude Muzerelle, Jean Paul Rio, Christine Métin, and Patricia Gaspar

Institut National de la Santé et de la Recherche Médicale, U616, and University Paris 06, Hôpital Pitié Salpêtrière, Institut Féderatif Neurosciences, F-75013 Paris, France

The calcium-stimulated adenylate cyclase 1 (AC1) has been shown to be required for the refinement of the retinotopic map, but the mechanisms involved are not known. To investigate this question, we devised a retinotectal coculture preparation that reproduces the gradual acquisition of topographic specificity along the rostrocaudal axis of the superior colliculus (SC). Temporal retinal axons invade the entire SC at 4 d *in vitro* (DIV) and eliminate exuberant branches caudally by 12 DIV. Temporal and nasal axons form branches preferentially in the rostral or caudal SC, respectively. Retinal explants from AC1-deficient mice, AC1$^{brl/brl}$, maintain exuberant branches and lose the regional selectivity of branching when confronted with wild-type (WT) SC. Conversely, WT retinas correctly target AC1$^{brl/brl}$ collicular explants. The effects of AC1 loss of function in the retina are mimicked by the blockade of ephrin-A5 signaling in WT cocultures. Video microscopic analyses show that AC1$^{brl/brl}$ axons have modified responses to ephrin-A5: the collapse of the growth cones occurs, but the rearward movement of the axon is arrested. Our results demonstrate a presynaptic, cell autonomous role of AC1 in the retina and further indicate that AC1 is necessary to enact a retraction response of the retinal axons to ephrin-A5 during the refinement of the retinotopic map.

Key words: **adenylate cyclase; ephrin; retinal map; axon branching; presynaptic mechanisms; knock-out mice; development; retraction; retinotectal; retina; growth cone; cAMP**

Introduction

Establishing topographic maps in the nervous system involves a period of axon remodeling when exuberant projections are shaped to restricted axon terminal arbors (Holt and Harris, 1998; Luo and O'Leary, 2005). The retinotectal system is a favorite model to analyze the mechanisms involved in this restructuring. Although a large number of players have been identified, such as neuronal activity, neurotransmitters, neurotrophins, or molecular guidance cues, their respective contribution and intricacies are unclear (Goodhill and Richards 1999; Cline, 2003; McLaughlin et al., 2003a).

In rodents, the embryonic retinal axons initially invade the entire superior colliculus (SC) with limited topographic specificity. Subsequently, overextended axon branches are removed, and collateral branches establish a focused and precise axon terminal arbor (Sachs et al., 1986; Simon and O'Leary, 1992). Membrane-bound guidance molecules ephrin-As and their EphA receptors in the retina define the target zones in the SC and are required for establishing the retinal topography along the rostrocaudal axis (Knoll and Drescher, 2002; McLaughlin et al., 2003a).

Altered refinement of the retinocollicular map was described in several mouse mutants with altered neurotransmission properties: the monoamine oxidase A knock-out (MAOA-KO) mice (Upton et al., 1999), the serotonin transporter knock-out (SERT-KO) mice (Upton et al., 2002), the nicotinic β2 receptor KO mice (McLaughlin et al., 2003b), and the adenylate cyclase 1 (AC1)-deficient mice (Ravary et al., 2003). A similar phenotype was noted in all four KO mice, comprising a lack of retraction of the exuberant projections from the ipsilateral eye and altered refinement of the topographic maps with enlarged axon terminal zones. In the MAOA-KO and SERT-KO mice, the abnormalities were linked to the presynaptic 5-HT$_{1B}$ receptor, which inhibits glutamate release at the retinotectal synapse (for review, see Gaspar et al., 2003). In the nicotinic β2 receptor KO, altered spontaneous firing patterns in the retina were correlated to the targeting abnormalities (McLaughlin et al., 2003b).

In the AC1-deficient mice, the mechanisms involved remain controversial. It is unclear whether the AC1 gene (ADCY1) is required presynaptically (Ravary et al., 2003) or postsynaptically (Plas et al., 2004) and whether AC1 acts by modulating synaptic plasticity (Xia and Storm, 1997; Lu et al., 2003) or by modulating trophic responses of the retinal axons. Changes of the levels of cAMP in the growth cones have direct effects on the growth of axons (Mattson et al., 1988; Lohof et al., 1992) and on their response to secreted chemotropic guidance signals (Song et al., 1998).

Received Aug. 11, 2005; revised Nov. 22, 2005; accepted Nov. 23, 2005.

This work was supported by grants from Institut National de la Santé et de la Recherche Médicale, "Retina France," and "Fondation de France." X.N. is supported by a grant from the Délégation Générale pour l'Armement. We thank Serge Marty, Luc Maroteaux, Alexandra Rebsam, and Constantino Sotelo for critical reading of this manuscript at different stages. We thank Egbert Welker for the gift of the barrelless mouse strain and Pierre Vanderhaeghen for introducing us to the world of ephrins. We thank Claude Marie Bachelet from the imaging facility of Institut Féderatif Neurosciences for her assistance for the videomicroscopic analyses.

Correspondence should be addressed to Patricia Gaspar, Pavillon Enfance et Adolescence, Hôpital Pitié Salpêtrière, 47 Boulevard de l'Hôpital, 75651 Paris Cedex 13, France. E-mail: gaspar@infobiogen.fr.

DOI:10.1523/JNEUROSCI.3385-05.2006

 0270-6474/06/260862-11$15.00/0

To determine the site of action of AC1 in the retinotectal system, we established an organotypic coculture that reproduces the late stages of development of the retinal projection. By combining different genotypes of retinal and collicular explants, we demonstrate that AC1 is required in the retina and not in the SC for the remodeling of the retinal axons. We found that the lack of AC1 causes topographic alterations of the retinal projection by preventing regionally selective branching and retraction of exuberant branches. These effects are mimicked by a blockade of ephrin-A5 signaling. Furthermore, the full collapse response of retinal axons to ephrin-A5 requires the presence of AC1 in the retinal axons.

Materials and Methods

Pregnant mice and pups were purchased from Janvier or obtained from local colonies. The plug date was defined as embryonic day 0.5 (E0.5), and the date of birth was defined as as postnatal day 0 (P0). Wild-type (WT) mice were maintained on a Swiss background (OF1). In the enhanced green fluorescent protein (eGFP) mouse strain that we used, the expression of eGFP is controlled by a chicken β-actin promoter (Hadjantonakis et al., 1998). The *brl* mutation occurred spontaneously in the *nor* strain (Welker et al., 1996) in a breeding stock of the Department of Anatomy at the University of Lausanne (Lausanne, Switzerland), and it has been subsequently characterized as an insertion of a retrotransposon in the AC1 gene (Abdel-Majid et al., 1998). The loss of AC1 function in this mouse strain was shown by the reduction of calcium-stimulated adenylate cyclase activity in total brain extracts (Abdel-Majid et al., 1998) in the SC and in the retina (Ravary et al., 2003). They will hence be termed $AC1^{brl/brl}$ to distinguish them from the mice with a homologous recombination in the Adcy1 gene (Villacres et al., 1995). The $AC1^{brl/brl}$ mice were crossed with the actin eGFP strain to obtain a line homozygous for the *brl* mutation and heterozygous for the actin-eGFP transgene.

Organotypic cocultures

After decapitation, the brains of P6 pups were dissected in cold PBS-0.5% glucose. The brainstem was separated from the forebrain, and a block containing the superior and inferior colliculus (IC) was sliced into 300-μm-thick parasagittal slices using a McIlwain tissue chopper. Two parasagittal slices were taken from the central part of each colliculus, transferred on a Millicell culture insert with 0.4 μm pore size (Millipore, St Quentin en Yvelines, France), and maintained in 5% CO_2 at 35°C. E15.5 embryos expressing eGFP were obtained from pregnant WT or $AC1^{brl/brl}$-eGFP mice. The nasal retina was marked before removing the eye for orientation. The retinas were extracted and placed in PBS-glucose. They were dissected into three tiers: nasal, central, and temporal. The nasal and temporal third were collected separately and then cut into 200-μm-square explants. Individual retinal explants were placed rostral to the mesencephalic parasagittal slices. These preparations were then cultured for 4, 7, or 12 d. The culture medium (60% basal medium eagle, 20% inactivated horse serum, 20% 1× HBSS, 0.4% glucose, 0.8 mM glutamine) was replaced every 2 d. In the experiments in which ephrin-A signaling was inhibited, ephrin-A5-Fc or EphA3-Fc (2 μg/ml; R & D Systems, Lille, France) was added the day after the beginning of the culture and at each change of the medium.

For single reconstructions of retinal axons, we created retinal chimeras in which very small (<50 μm) fragments of eGFP-expressing retinas were mixed to larger (~200 μm) unlabeled retinal explants. The eGFP and the non-eGGP retinas were taken from littermates, creating either WT/WT_{GFP} or $AC1^{brl/brl}/AC1^{brl/brl}{}_{GFP}$ chimeras.

Collapse assay

Retinal explants from E14.5 eGFP mouse embryos were cultured on poly-L-lysine-laminin-coated coverslips for 24 h in DMEM/F-12 medium [DMEM/F12 (Invitrogen, Cergy-Pontoise, France), 1 mM glutamine (Invitrogen), 0.01% BSA (ICN Biomedicals, Strasbourg, France), 1% penicillin (Invitrogen)]. After 24 h, ephrin-A5-Fc (250 ng/ml) was added to the culture medium, and the cultures were fixed 30 min later, rinsed, and immunostained with anti-GFP. The same assay was conducted with videomicroscopy using a medium supplemented with sodium pyruvate (1 mM) and HEPES (20 mM) in a chamber maintained at 37°C. The growth cones were filmed during 1 h before and 2 h after ephrin-A5 bath application (one image/min at a 40× power objective; inverted microscope, phase contrast; Zeiss, LePecq, France). Morphometric analyses and films were done using the MetaMorph software. We measured the velocity of the growth and of the retraction movements by recording the distance traveled by the cones during the 30 min periods that preceded or followed the application of the reagents.

Immunostaining

Cultures were fixed in 4% paraformaldehyde, with 15% sucrose for 2 h at room temperature, washed for 1 h in PBS-0.2% gelatin and 0.25% Triton X-100, and incubated overnight in rabbit anti-GFP antibody (1/1000; Invitrogen). They were washed again and incubated for 2 h in an anti-rabbit antibody coupled to Alexa 488 fluorochrome (1/200; Invitrogen). The coculture preparations were counterstained for 10 min with bisbenzimide (10 μg/ml; Sigma, St Quentin en Yvelines, France). The collapse assay and coculture preparations were finally washed in PBS and mounted in mowiol-Dabco (25 mg/ml).

Electron microscopy

Cultures were fixed in increasing dilutions of 4% paraformaldehyde in the culture medium (1:4, 1:1, 4:1; 5 min each), followed by full-strength fixative (2 h), rinsed in PBS (1 h), and incubated overnight in anti-GFP antiserum (1/10,000) with 0.025% Triton X-100. DAB revelation was performed. Cocultures were postfixed for 2 h in 2% phosphate-buffered osmic acid, stained *en bloc* with uranyl acetate, dehydrated in graded series of ethanol, cleared in acetone, and flat-embedded in Araldite. Thick epoxy sections (1 μm) were cut to localize the retinorecipient tectal layer, which was then thin sectioned, before examination with a Philips CM 100 electron microscope.

Analysis and quantifications

Measures of the area covered by the retinal axons in the mesencephalic explants. This was done on the coculture experiments in which the entire retinal explant was eGFP labeled. For each experimental condition, we quantified 6–15 different cocultures from three independent experiments. Controls were included in each independent experiment. To avoid subjective biases in the measures, all of the cocultures were coded with numbers and decoded after the quantification process was over. A computerized image of each coculture was constructed for both the GFP and the bisbenzimide staining. This implies for each culture the acquisition of 30 image frames per staining (resolution 1280 × 1024 pixels) that were acquired with a Zeiss photomicroscope (10× objective), and a large video image of the culture (retaining the original resolution of the acquisition) was reconstructed using the MetaMorph software (Roper Scientific, Evry, France). Two types of grids were overlaid on these reconstructed video images. Grid1 (supplemental Fig. C, available at www.jneurosci.org as supplemental material) is a rectangular grid formed by 20 vertical and five horizontal lines allowing the definition of five dorsoventral bins (D1, D2. . . D5) and 20 rostrocaudal bins (R'1, R'2. . . R'20). Grid2 (supplemental Fig. D, available at www.jneurosci.org as supplemental material) was made by tracing a line along the upper border of the SC and delimiting 20 rectangular regions below this line (R1, R2. . . R20). The rostrocaudal measures obtained with these two types of grids were comparable.

On each reconstructed image (supplemental Fig. A, available at www.jneurosci.org as supplemental material), an inclusive threshold was set to include all or a large majority of the eGFP-labeled axons in the slice (supplemental Fig. B, available at www.jneurosci.org as supplemental material). The 0 was set as the background level in the slice in a region where no labeled retinal fibers were visible. Using this threshold, the number of pixels covered by the retinal axons was measured within each rectangle of the two grids. Because the size of the rectangles varies slightly in Grid2, the pixel counts obtained in each bin were expressed as the percentage (p) of the bin size. To normalize the values with respect to the size of the explant, the p value for each bin was expressed as the percentage of the sum of the p values in the entire grid (this value represents the fraction of the total area covered by the retinal axons in one bin).

Statistical measures were done using the Mann–Whitney *U* test on cumulated index frequencies along the rostrocaudal axis of the collicular explants.

Measures of the branching index of the retinal axons in different regions of the mesencephalic explant. This was done on the coculture preparations with retinas that comprise only a few eGFP-labeled axons (retinal chimeras of unequal sizes), allowing partial reconstructions of single eGFP-labeled axons to be done. All of the cocultures were number-coded to mask the experimental situation. Microscopic fields (350 × 275 μm) were acquired on a Leica (Nussloch, Germany) photomicroscope (40× objective) in the rostral and caudal halves of the SC and in the ventrorostral portion of the slice. One to four axon segments that were present in these microscopic fields were redrawn on the computer screen combining several acquisitions at different depths of the slice to image the branch ramifications. The length of these axon segments and the number of branches were then measured using MetaMorph software. After decoding these numbers to a given experimental condition, comparisons between genotypes and ages was done using the unpaired Student's *t* test.

Single retinal ganglion cell axon reconstructions. Complete reconstructions of single retinal axons, from the retinal explant to the axon terminal zone, were possible in 4–10 cases for the WT/WT and *brl*/WT cocultures at 4 and 12 d *in vitro* (DIV). The reconstructions were done by analyzing the cultures with a 40× objective: images were collected all along the trajectory of the retinal axons. The successive images were then pasted into a single image file using Photoshop (Adobe Systems, San Jose, CA) and imported to Adobe-Illustrator (Adobe Systems) in which the axons were redrawn.

Results

Characterization and validation of an organotypic retinotectal coculture model

The retinal projections to the SC are organized along a nasotemporal axis in the retina: retinal ganglion cells (RGCs) from the temporal part of the retina project rostrally in the SC, and nasal RGCs project caudally in the SC. To reproduce this topographic organization *in vitro*, retinal explants were microdissected from the nasal and temporal tiers of retinas and confronted to parasagittal slices of the mesencephalon. The use of retinas from actin-eGFP mice (Hadjantonakis et al., 1998) allowed us to visualize retinal ingrowth in the mesencephalic explant using GFP immunocytochemistry.

A progressive targeting of the SC by retinal axons was observed in the slice. During the first 4 DIV, the retinal axons grew within the entire mesencephalic slice (Fig. 1*A*,*B*), and all of the RGC axons were tipped by growth cones (Fig. 2*A*) that were oriented in all directions, indicating that

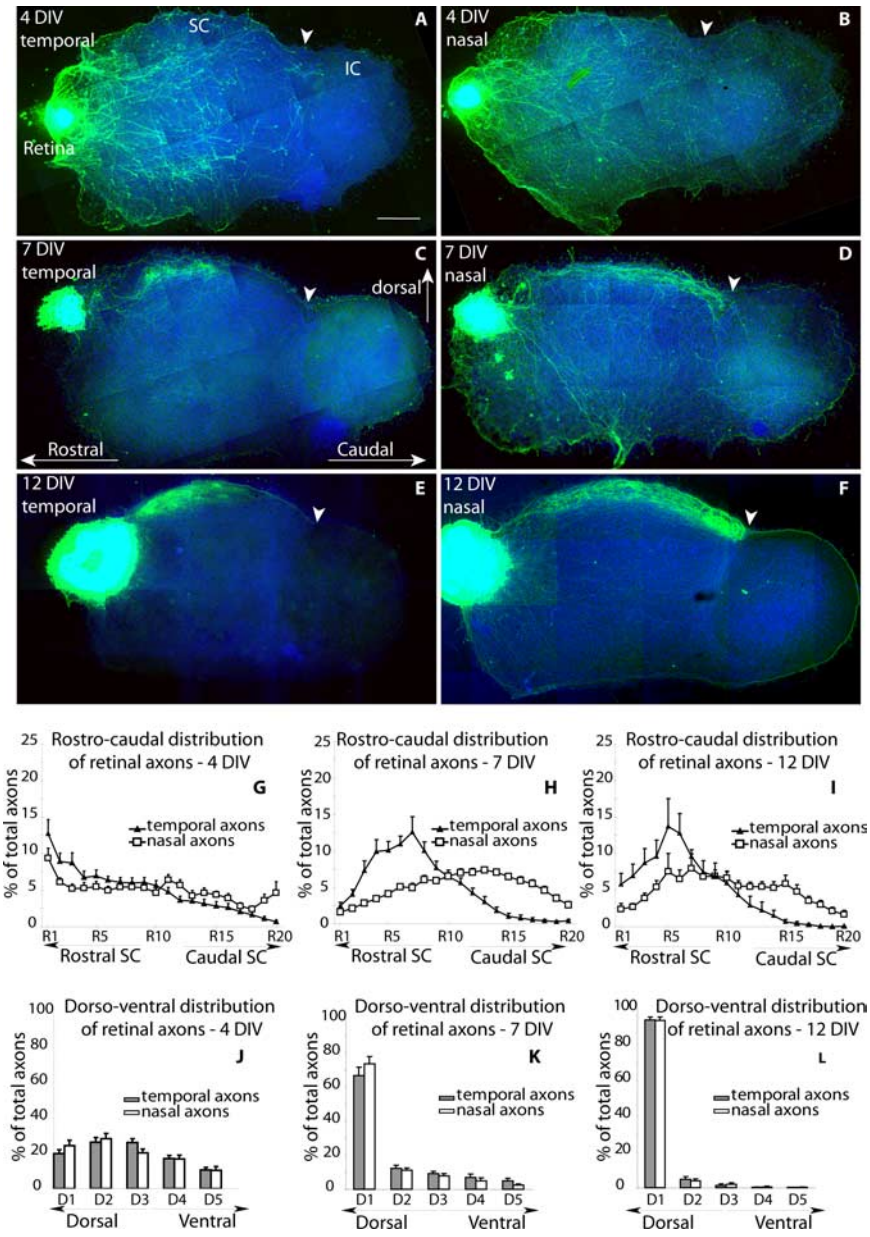

Figure 1. Progressive acquisition of target selectivity in an organotypic retinotectal coculture. ***A–F***, Temporal (***A***, ***C***, ***E***) or nasal (***B***, ***D***, ***F***) retinal explants were dissected from E15.5 eGFP-expressing embryos and positioned rostral to WT parasagittal slices of the mesencephalon taken from P6 pups. Cultures were fixed after 4 DIV (***A***, ***B***), 7 DIV (***C***, ***D***), or 12 DIV (***E***, ***F***). In all of the reconstructed micrographs, rostral is to the left, dorsal is up, and the frontier between the SC and the IC is marked by an arrowhead. Scale bar, 500 μm. ***A***, ***B***, At 4 DIV, temporal (***A***) and nasal (***B***) GFP-immunolabeled retinal axons indifferently invade the dorsal and ventral mesencephalic slice, extending into the IC. ***C***, ***D***, At 7 DIV, a majority of temporal (***C***) and nasal (***D***) retinal axons terminate in the dorsal part of the slice, and fewer axons remain in the ventral mesencephalon. Temporal axons become concentrated in the rostral half of the SC (***C***), whereas nasal retinal axons extend to the caudal border of the SC (arrowhead), with a few axons remaining in the IC. ***E***, ***F***, At 12 DIV, temporal (***E***) and nasal (***F***) retinal axons are concentrated in a narrow layer in the dorsal part of the mesencephalic explant. Temporal axons form a dense axon terminal arbor that is limited to the rostral SC (***E***), and nasal axons form a continuous rostrocaudal band in the SC, which stops at the SC/IC frontier (***F***). A somewhat denser terminal plexus is noted caudally. ***G–I***, Quantification of the surface occupied by labeled retinal axons along the rostrocaudal axis. Pixels occupied by labeled axons were measured in equally spaced rostrocaudal bins (R1, R2. . . R20) (supplemental figure, available at www.jneurosci.org as supplemental material) along the rostrocaudal axis of the SC and are expressed as a percentage of the total labeled axons for each slice. The mean values and SEM were calculated at 4 DIV (***G***) (nasal explants, $n = 10$; temporal explants, $n = 14$), 7 DIV (***H***) (nasal explants, $n = 18$; temporal explants, $n = 14$), and 12 DIV (***I***) (nasal explants, $n = 12$; temporal explants, $n = 9$). A statistical difference between the distribution of the temporal and retinal was found at 7 and 12 DIV ($p < 0.05$; Mann–Whitney *U* test) but not at 4 DIV. ***J–L***, Quantification of the retinal axons along the dorsoventral axis of the slice. Pixels occupied by the labeled axons were measured in dorsoventral bins (D1, D2. . . D5) and are expressed as a percentage of the total surface covered by axons. The histograms show the mean values at three different times: 4 DIV (***J***) (nasal explants, $n = 10$; temporal explants, $n = 14$), 7 DIV (***K***) (nasal explants, $n = 18$; temporal explants, $n = 14$), and 12 DIV (***L***) (nasal explants, $n = 12$; temporal explants, $n = 9$). The error bars indicate SEM.

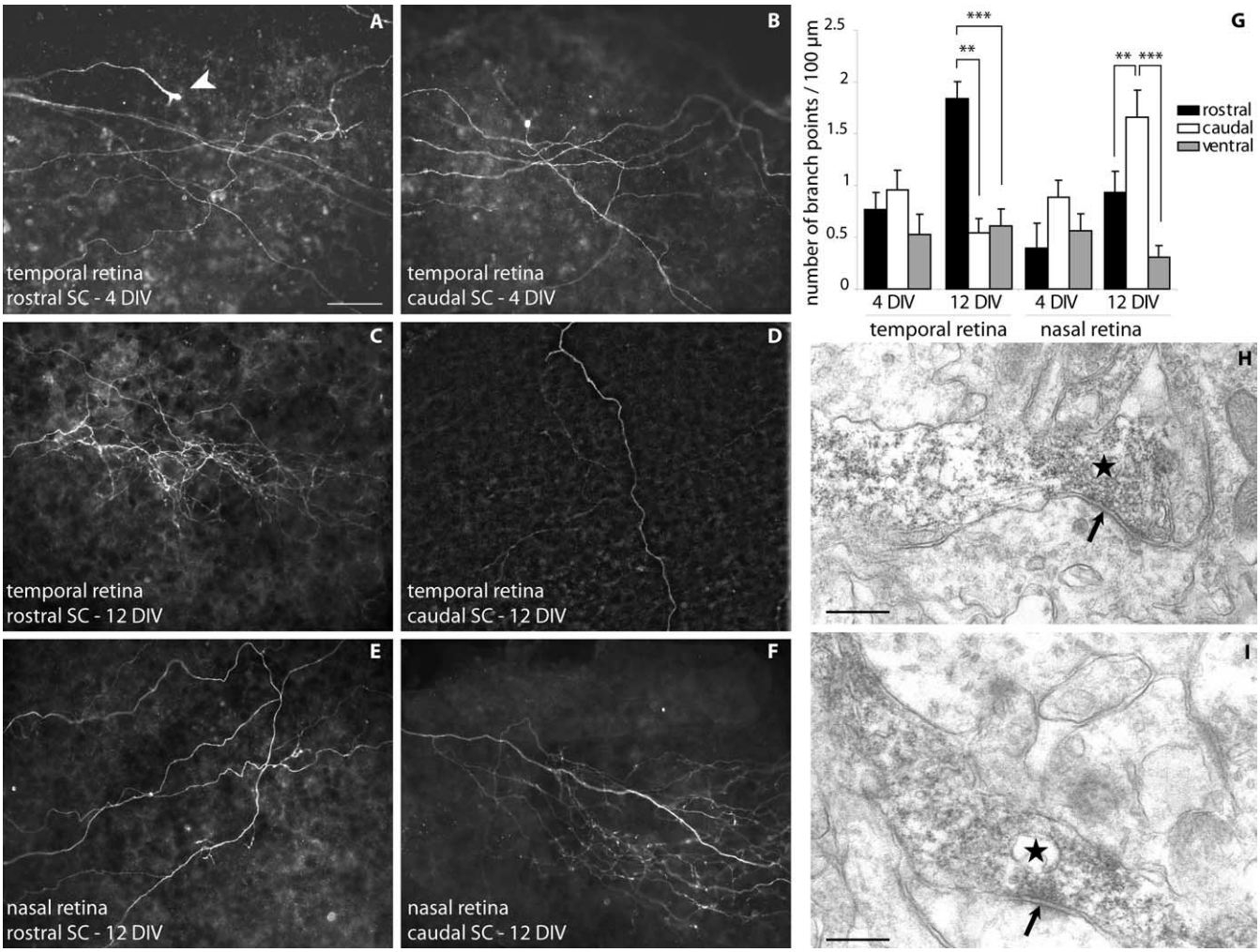

Figure 2. Regionally selective axon branching and synaptogenesis in the coculture. Axon branching was analyzed in cocultures in which the retinal explants contained a small number of GFP-labeled retinal cells. This showed a progressive elaboration of complex axon branches that was regionally selective by 12 DIV. ***A***, ***B***, At 4 DIV, the temporal retinal axons elongate in the rostral (***A***) and caudal (***B***) halves of the SC. A few simple branches are observed, and the axon terminals are tipped with growth cones (arrowhead). ***C***, ***D***, At 12 DIV, the temporal retinal axons form complex axon terminals in the rostral half of the SC (***C***), and only rare axons with few branches are found in the caudal half of the SC (***D***). ***E***, ***F***, At 12 DIV, nasal retinal axons course in the rostral SC (***E***) where they form fewer branches than in the caudal part of the SC (***F***). Scale bar, 50 μm. ***G***, Quantifications of the linear branching density of the retinal axons in three regions of the slice, rostral half of the SC (black), caudal half of the SC (white), and ventral mesencephalon (gray) at 4 and 12 DIV. The means and SEM were calculated from measures made on 10–20 different reconstructed axons for each region and condition. $^{**}p < 0.01$, $^{***}p < 0.001$; unpaired Student's *t* test. ***H***, ***I***, Two examples of GFP-immunopositive retinal terminals (asterisks) establishing an asymmetric synaptic contact with a collicular dendrite (arrow). Scale bar: ***A–C***, 20 μm; ***D–F***, 250 nm.

the elongating axons randomly explore the mesencephalic slice, including the nontarget areas such as the ventral mesencephalon and the inferior colliculus. At 7 DIV, the number of exuberant retinal axons in the ventral mesencephalon and the inferior colliculus had decreased substantially (Fig. 1*C*,*D*), and they were no longer observed at 12 DIV, when the retinal axons became concentrated in a narrow band in the dorsal portion of the mesencephalic slice (Fig. 1*E*,*F*). To estimate this redistribution of axons toward the optic SC, we quantified the surface area occupied by the labeled retinal axons in five bins from dorsal (D1) to ventral (D5) (supplemental Fig. C, available at www.jneurosci.org as supplemental material). The D1 bin approximately corresponds to the optic layers of the SC. At 4 DIV, 22% of the temporal and nasal retinal axons were located in D1 (Fig. 1*J*). The proportion increased to 69% at 7 DIV (Fig. 1*K*) and to 95% at 12 DIV (Fig. 1*L*).

Concurrently, a progressive targeting of the temporal retinal axons to the rostral half of the SC was observed (Fig. 1*A*,*C*,*E*). At 4 DIV, the growth pattern of the retinal axons emerging from the nasal or temporal explants was similar: the axons invaded the entire rostrocaudal length of the SC (Fig. 1*A*,*B*). However, a systematic redistribution of the temporal retinal axons to the rostral half of the SC became visible, when the cultures were maintained beyond 1 week (Fig. 1*C*,*E*). In contrast, the nasal retinal fibers remained more evenly distributed across the rostrocaudal axis (Fig. 1*D*,*F*). To evaluate this regional redistribution, 20 equally spaced bins were drawn along the rostrocaudal axis of the SC (from R1 rostral to R20 caudal) (supplemental Fig. D, available at www.jneurosci.org as supplemental material). These measures revealed a consistent and reproducible change in the distribution of the temporal retinal axons over time. At 4 DIV, an equal amount of temporal retinal axons were present in the rostral (Σ_R = R1 + R2 + . . . R10) and caudal (Σ_C = R11 + R12 + . . . R20) halves of the SC (50%) (Fig. 1*G*). As the cultures matured, a highly skewed distribution became visible. At 7 DIV, 82% of the temporal axons became localized in the rostral half of the SC (Fig. 1*H*), and this percentage increased to 95% at 12 DIV (Fig. 1*I*). These measures indicate that a retraction of the temporal retinal

axons from the caudal part of the SC occurs between 4 and 12 DIV.

In addition to the elimination of the ectopically localized axons in the slice, a regionally selective branching pattern was observed. At 4 DIV, a majority of the retinal axons were branchless (Fig. 2*A*,*B*), with few axons displaying simple first-order branches. The extremities of all of these simple or branched axons were tipped with growth cones (Fig. 2*A*). To determine whether axon branching is topographically focused, the density of branch points per unit axon length was estimated. At 4 DIV, the linear branch density of the nasal and the temporal retinal axons was not significantly different in the rostral and caudal halves of the SC and in the rostroventral quadrant of the slice (Fig. 2*G*). At 12 DIV, complex retinal branches were observed in the SC (Fig. 2*C*,*F*); the collateral branches became almost exclusively confined to the superficial portion of the slice with rare axons in the ventral portion of the explant (Fig. 3*B*,*C*). Branch density estimates showed that temporal retinal axons formed at least three times more branches in the rostral versus the caudal halves of the SC; conversely, nasal retinal axons formed twice as many branches in the caudal versus the rostral halves of the SC (Fig. 2*G*). Thus, the analysis of axon branching revealed a regional preference of the temporal and nasal retinal axons for their appropriate targets in the rostral or caudal halves of the SC, respectively.

Complete reconstructions of single retinal axons at 4 DIV showed different profiles of retinal axons: some fibers extended over a large part of the explant, whereas others had shorter and simpler trajectories (four examples of 10 complete single axon reconstructions are shown in Fig. 3*A*). At 12 DIV, single axons were found to have either direct or convoluted routes toward their terminal target zones (Fig. 3*C*), where they formed complex ramifications. The nasal and temporal axons formed restricted axon arbors along the rostrocaudal axis (Fig. 3*B*,*C*), temporal retinal arbors were always localized in the rostral half of the SC (Fig. 3*B*), and the position of the nasal retinal axon arbors varied from a central to a caudal position in the SC (Fig. 3*C*).

To determine whether a normal synaptic maturation occurs in the slice *in vitro*, we analyzed the ultrastructure of the cocultures at 12 DIV. Based on morphological criteria that described the synaptogenesis in the SC (Lund and Lund, 1972; Sachs et al., 1986), we identified symmetric, asymmetric, and serial synapses in the SC (data not shown). In addition, using GFP-immunocytochemistry to label the retinal axons, retinotectal synapses were identified between the retinal axons and dendrites of collicular neurons (Fig. 2*H*,*I*). Synaptic junctions were observed on 30% of the 120 axon terminal profiles examined in the culture at 12 DIV.

In conclusion, the coculture assay that we developed reproduces the topographic specificity of the temporal retinal axons for the rostral part of the SC, with a gradual emergence of topographic specificity of the retinal axon arbors that is mediated by focused branching and elimination of exuberant retinal axons.

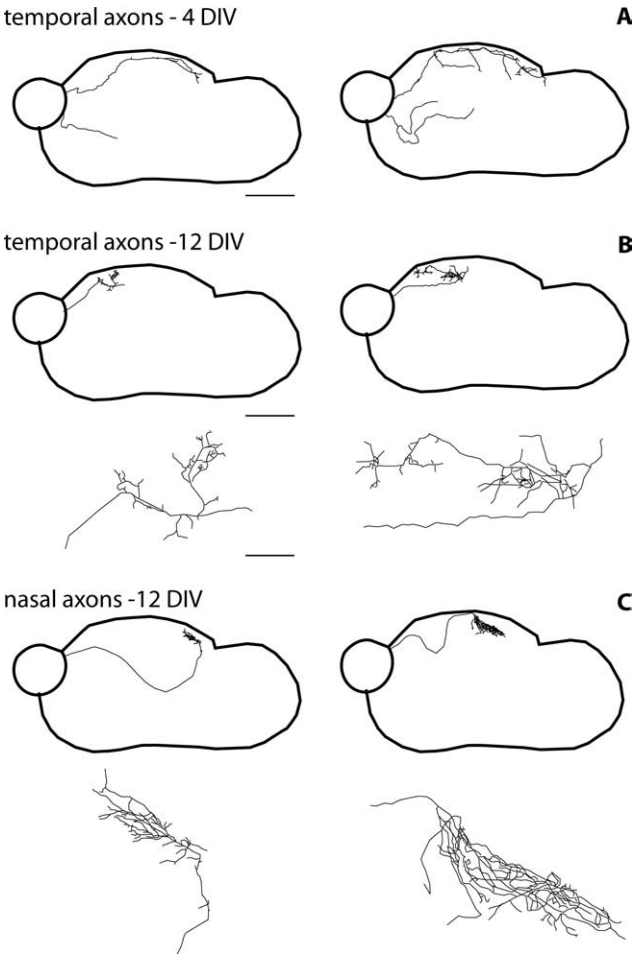

Figure 3. Single-axon reconstructions show the progressive laminar and regional targeting of the retinal axons and an increased complexity of axon terminal arbors. The entire trajectory of the axon was traced from its origin to its termination point (40× objective) in cases in which a few GFP retinal cells were integrated to a larger unlabeled retinal explant. The reconstructed axon arbor was then reduced for representation. The position of the axons in the slice is shown in the top part of the panels, and the terminal arbor is illustrated in the bottom part of the panels. Scale bar: top, 600 μm; bottom, 100 μm. ***A***, At 4 DIV, the temporal retinal axons are either simple or they form primary branches at different rostrocaudal locations within the SC and in the ventral portion of the mesencephalic slice (4 axons of 7 complete reconstructions are shown). ***B***, ***C***, At 12 DIV, collateral branches are formed almost exclusively in the superficial part of the slice and the individual arbors cover a limited portion of the SC. Temporal axons arborize selectively in the rostral half of the SC (2 examples out of 10 reconstructed axons are shown) (***B***). Nasal axons form complex axon terminal arbors in the caudal or at midlevels of the SC (2 examples are shown out of 10 reconstructed axons) (***C***). An example of an axon reaching its target after a convoluted ventral loop is illustrated in the left side of the panel.

Ephrin-A signaling is required for the topographic mapping of temporal retinal axons in the coculture

The differential response of the nasal and temporal retinal axons in the coculture is consistent with previous observations of retinal growth on striped carpets prepared from tectal membranes, in which retinal axons show an ephrin-A-dependent preference for anterior tectal membranes (Ciossek et al., 1998). Because graded ephrin-A expression in the SC is maintained over protracted postnatal periods (Rodger et al., 2001), we questioned whether ephrin-A signaling is involved in the targeting of the temporal retinal axons in the organotypic cocultures. To investigate this, we blocked ephrin-A signaling by a soluble extracellular domain of the receptor EphA3-Fc (2 μg/ml), which acts as a competitive inhibitor of the endogenous receptors or by using an excess of the ligand ephrin-A5-Fc (2 μg/ml) (Ciossek et al., 1998). In the treated cocultures ($n = 30$ for ephrin-A5; $n = 24$ for EphA3; $n = 9$ controls), the temporal retinal axons occupied the entire rostrocaudal extent of the SC (Fig. 4*C*), contrasting with the distribution of the temporal retinal axons in the control conditions (Fig. 4*A*). Quantifications of the temporal retinal axon distribution in the control and experimental situations confirmed the statistical significance of this change (Fig. 4*E*,*F*). Although no

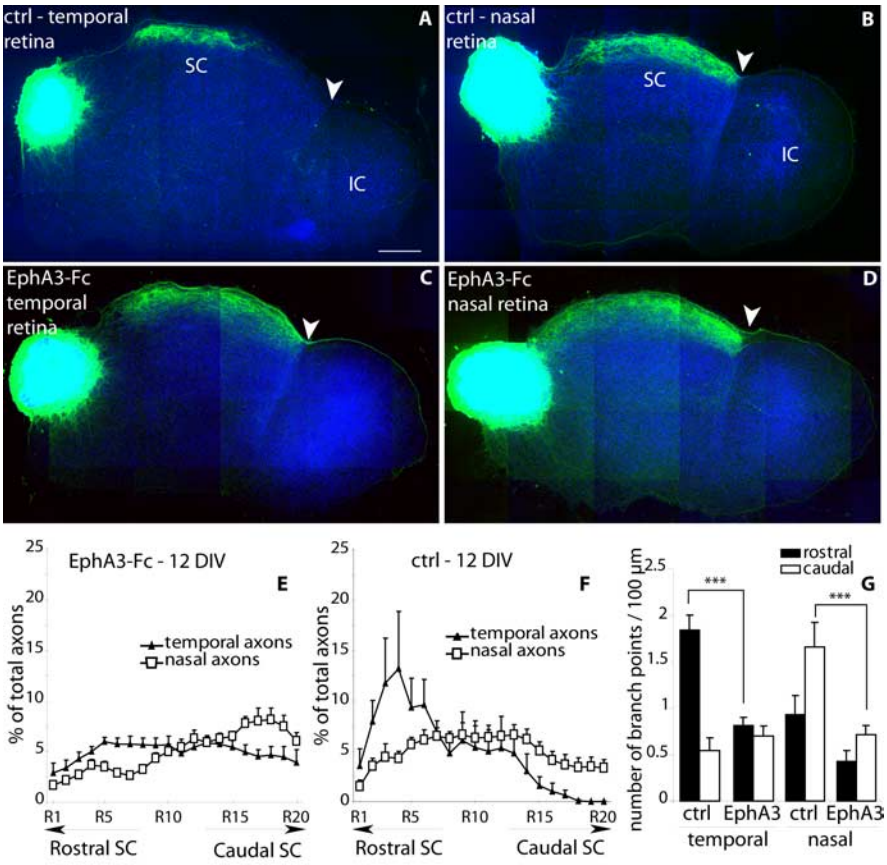

Figure 4. Ephrin-A signaling is necessary for the rostral targeting of the temporal retinal axons. ***A–D***, Retinal explants from the temporal (***A***, ***C***) or nasal (***B***, ***D***) tiers of the retina were cultured facing mesencephalic slices and grown in control media (***A***, ***B***) or with the addition of EphA3-Fc (***C***, ***D***). The cocultures were fixed after 12 DIV and immunostained with eGFP. Temporal retinal axons terminate as a dense plexus in the rostral half of the SC in the control condition (***A***) and form a continuous dense band that extends to the IC border in the EphA3-treated condition (***C***). Nasal retinal axons display a similar distribution along the SC in the control (***B***) and EphA3-treated condition (***D***). Scale bar, 500 μm. ***E***, ***F***, Graphs measuring the rostrocaudal distribution of the temporal and nasal retinal axons. In the Eph-treated condition, the distribution curve of the nasal and temporal curves are not statistically different (***E***). In the control condition, there is a significant difference between the nasal and temporal distributions ($p < 0.05$; Mann–Whitney *U* test) (***F***). The values are expressed as a percentage of the total surface occupied by the labeled axons, in consecutive bins (R1 to R20) along the rostral to caudal axis of the SC. ***G***, Quantification of the linear branching density in two regions of the slice (rostral, black; caudal, white) in control and EphA3-Fc conditions at 12 DIV. Branching density is uniform in EphA3-treated cultures contrasting with the regional branching difference in the controls. Error bars represent SEM. ***$p <$ 0.001; Student's *t* test. ctrl, Control.

changes in the distribution of the nasal retinal axons were observed when all of the retinal fibers were labeled (Fig. 4*B*,*D–F*), single axon analyses indicated a loss of regionally selective branching of both the nasal and temporal axons, as well as a reduced number of axon branches (Fig. 4*G*).

These experiments indicate that ephrin-A signaling is involved in the rostral targeting of the temporal retinal axons terminals in the coculture assay.

Adenylate cyclase 1 is required in the retina for axon terminal remodeling

We have shown previously abnormalities in the refinement of the retinogeniculate and retinotectal map in mutants of the AC1$^{brl/brl}$ mouse strain (Ravary et al., 2003). To determine whether AC1 is required in the retina or in the SC, we cocultured retinal explants from the AC1$^{brl/brl}$ retinas with WT mesencephalic slices (Fig. 5*B*) and WT retinal explants with AC1$^{brl/brl}$ mesencephalic explants (Fig. 5*C*) in comparison with WT/WT cocultures (Fig. 5*A*).

At 4 DIV, the AC1$^{brl/brl}$ retinal axons invaded the entire explant, with a vigor that was comparable with that of WT retinal axons (data not shown), indicating that there are no intrinsic axon growth defects linked to the lack of AC1.

Differences between the WT and the AC1$^{brl/brl}$ axons became visible at 12 DIV, because the AC1$^{brl/brl}$ temporal retinal axons failed to retract from the caudal SC and covered the entire rostrocaudal extent of the SC (Fig. 5*B*). Quantifications of five *brl*/WT cocultures showed that this behavior was consistent and statistically different from that of WT/WT cocultures (Fig. 5*E*). We analyzed the trajectories of individual AC1$^{brl/brl}$ retinal axons at 12 DIV. Single axon reconstructions showed that the retinal AC1$^{brl/brl}$ axons had lost their regional branching selectivity. Temporal retinal axons maintained branches in the caudal half of the SC (Fig. 6*A*), and nasal retinal axons formed abnormal branches in the rostral SC and in the ventral mesencephalon (Fig. 6*B*). Moreover, a number of axonal terminals were still tipped with growth cones at 12 DIV, contrasting with the control situation, where growth cones have disappeared. The lack of selectivity of rostrocaudal branching was confirmed with quantitative estimates of the linear branching density. The branching index of the AC1$^{brl/brl}$ axons was similar in the rostral and caudal halves of the SC (Fig. 5*D*), although the total branch number was not modified.

In converse experiments, where the WT temporal or nasal retinas faced a mesencephalic explant from the AC1$^{brl/brl}$ mice, no detectable alteration in the distribution of the temporal retinal axons was found (Fig. 5*C*,*F*).

These experiments show that AC1 is required in the retina and not in the SC for the remodeling of the retinal axons, demonstrating a cell autonomous role of AC1 in the RGCs. Lack of AC1 does not modify the branching capacity of the axons but alters its regional selectivity. Furthermore, lack of AC1 interferes with the normal pruning back of exuberant retinal axons.

Loss of AC1 alters the axonal retraction induced by ephrin-A5

The abnormalities of retinal axon targeting that are observed in the AC1$^{brl/brl}$/WT coculture preparation could be linked to a defective retraction of exuberant retinal axons along the rostrocaudal axis of the SC in response to topographic guidance cues. The ephrin-As are reasonable candidates, because they mediate the retraction of temporal retinal axons from membrane-bound cues in the caudal SC (Walter et al., 1987; Ciossek et al., 1998) and in the present coculture model. Furthermore, targeting abnormalities are found in the SC of mice lacking ephrin-A2/A5 (Frisen et al., 1998; Feldheim et al., 2000).

To test whether the repulsive effect of ephrin-As is modified in the mutant retinas, we used the retinal collapse assay using solu-

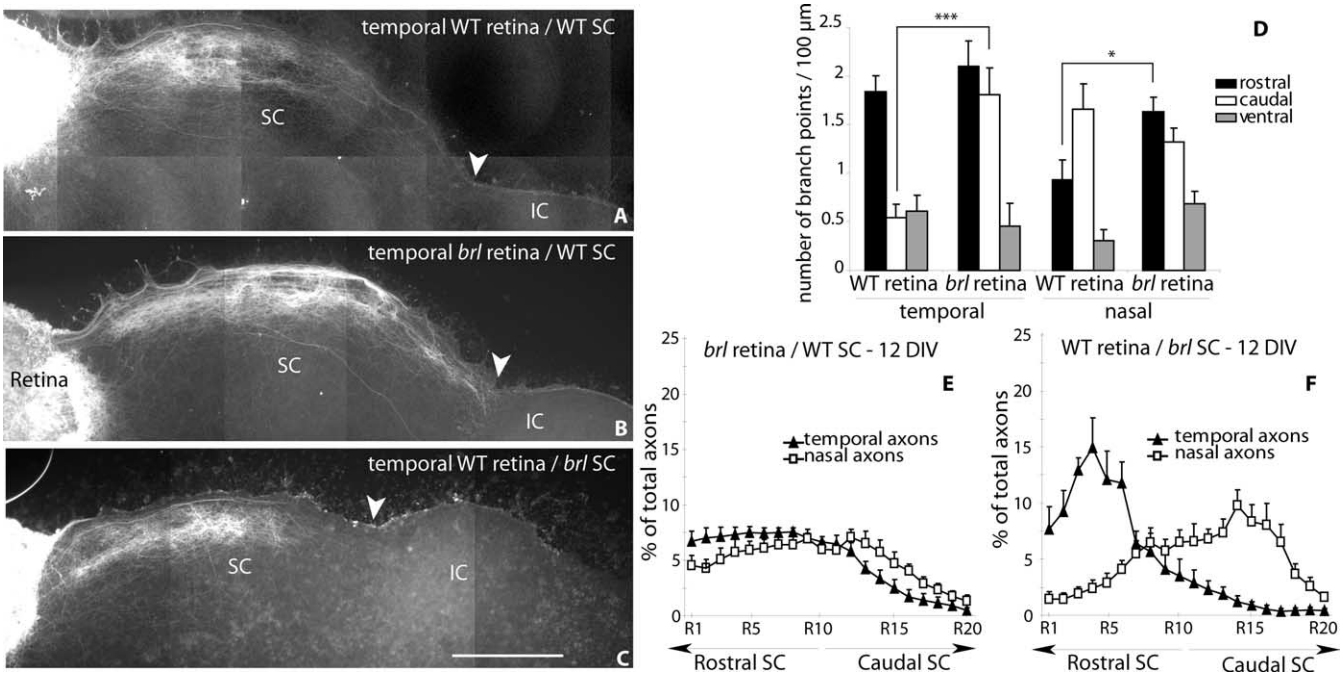

Figure 5. AC1 is required in the retina and not in the SC for topographic targeting of the temporal retinal axons. ***A–C***, Retinal explants from the temporal retinas of WT (***A***, ***C***) of AC1$^{brl/brl}$ (*brl*) were confronted to mesencephalic explants from WT (***A***, ***B***) or AC1$^{brl/brl}$ (***C***) and cocultured for 12 d. Control temporal explants grown in the same experiment show the restriction of the axon terminal arbors to the rostral half of the SC (***A***). The temporal AC1$^{brl/brl}$-eGFP retinas that are confronted to wild-type SC form an axon terminal network that covers the entire rostrocaudal extent of the SC up to the IC border. A few axons are seen coursing in the ventral portion of the mesencephalic explant (***B***). Temporal retinal explants from WT-eGFP retinas that are confronted to a mesencephalic slice of AC1$^{brl/brl}$ mice form a normal axon terminal network in the rostral half of the SC (***C***). Scale bar, 500 μm. ***D***, ***E***, Measures of the surface occupied by labeled temporal and nasal retinal axons along the rostrocaudal axis of AC1$^{brl/brl}$ retinas in WT mesencephalic explants (***D***) (temporal, $n = 12$; nasal, $n = 13$) and of WT temporal and nasal retinal axons in AC1$^{brl/brl}$ mesencephalic explants (***E***) (nasal, $n = 9$; temporal, $n = 7$). ***F***, Measures of linear branching densities of single WT and AC1$^{brl/brl}$ axons at 12 DIV. Branching density of the temporal *brl* retinal axons in the caudal SC is significantly increased in comparison to controls (***$p < 0.001$). Branching density of the nasal AC1$^{brl/brl}$ axons is increased in the rostral SC (*$p < 0.05$). Error bars represent SEM.

ble ephrin-A5 (Wahl et al., 2000). Because in such assays both the temporal and nasal retinal axons display similar collapse responses, the AC1$^{brl/brl}$ and WT retinal explants were prepared from the entire retina (comprising a mix of central, temporal, or nasal retinal explants) and grown for 24 h on laminin-coated coverslips. Measures of axon length showed no difference in the growth rates of the WT and the AC1$^{brl/brl}$ RGC axons (data not shown). Bath applications of ephrin-A5-Fc (from 1 ng/ml to 2 μg/ml; usual dose, 250 ng/ml) caused the collapse of 75% of the retinal growth cones, compared with 20% in the control condition (Fig. 7*B1*). No difference in the percentage of collapsing cones was found on explants from AC1$^{brl/brl}$ retinas (Fig. 7*B1*). However, a closer examination revealed morphological differences between the WT and the mutant retracting cones. WT collapsing cones generally had a single, long trailing process preceded by a retraction bulb (Fig. 7*A1*,*A2*), whereas the AC1$^{brl/brl}$ collapsing cones more frequently displayed two or three short trailing processes (Fig. 7*A3*). This was evaluated quantitatively by counting the number of retracted filopodia on collapsed growth cones and measuring the length of the longest trailing process 30 min after the application of the soluble ephrin-A5. These measures (100 cones from three independent experiments) showed a significant increase in the number of trailing filopodia in the AC1$^{brl/brl}$ condition (Fig. 7*B2*) and a 70% decrease in the length of the longest trailing process (Fig. 7*B3*).

Video microscopic studies of the collapse response allowed us to further characterize the altered response of the mutant retinal axons. In WT retinal axons growing on a laminin substrate at a velocity of 45 $\pm$ 5 μm/h, the application of ephrin-A5 caused a rapid collapse of the growth cone (Fig. 8*A*), which is followed by a rearward movement of the axon tip. The velocity of this rearward movement was calculated to be 150 $\pm$ 18 μm/h during the 30 min period that followed the application of ephrin-A5-Fc (Fig. 8*A*, *C*) (video 1, available at www.jneurosci.org as supplemental material). This rearward movement covered by the collapsing cone matched the length of the trailing profile on the fixed preparations (Fig. 7*A2*). In explants from AC1$^{brl/brl}$ retinas, the growth speed of the tracked axons before ephrin application was similar to that of WT axons (Fig. 8*C*) (video 1, available at www.jneurosci.org as supplemental material). This further stresses that AC1 is not required for normal axon growth. After the ephrin-A5-Fc application, a collapse of the lamellipodia was visible (Fig. 8*B*) (video 1, compare frames 3 and 17, available at www.jneurosci.org as supplemental material). However, the rearward movement of the cone was considerably diminished to 40 $\pm$ 19 μm/h (Fig. 8*B*) (video 1, 100 min, available at www.jneurosci.org as supplemental material). In fact, the mutant retinal axons were essentially arrested, with no filopodial activity, whereas the WT retinal axons continued their rearward retraction course (video 1, available at www.jneurosci.org as supplemental material). This altered movement of the cones was observed in 15 of the 16 tracked axons after ephrin-A5-Fc application. Thus, lack of AC1 in the retinal growth cone alters the response of axons to ephrin-A5 by arresting the rearward movement of the growth cone.

Implication of cAMP signaling in the altered response to ephrins

Our experiments show that the process of axon retraction in response to ephrin-A5 requires the presence of AC1 in the retinal

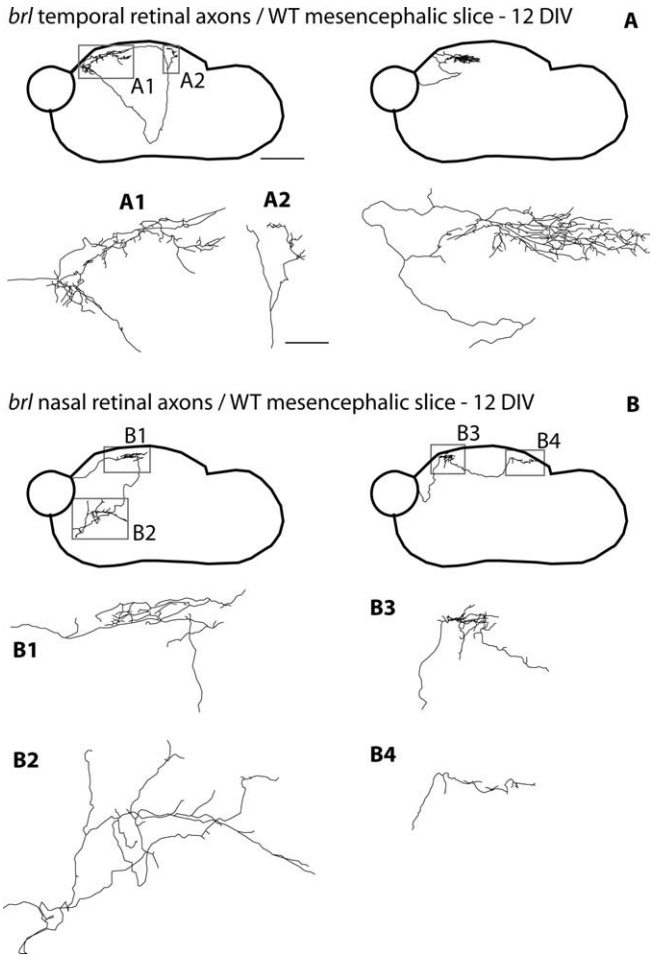

Figure 6. AC1$^{brl/brl}$ retinal axons maintain ectopic branches in the coculture. Single axons from AC1$^{brl/brl}$ mice were reconstructed as described (Fig. 3) at 12 DIV. Scale bar: top, 600 μm; bottom, 100 μm. ***A***, The temporal AC1$^{brl/brl}$ axons form complex terminal arbors in the superficial and rostral halves of the SC but, in addition, establish abnormal branches in the caudal part of the SC (***A2***) ($n = 5$ reconstructed axons). ***B***, Nasal AC1$^{brl/brl}$ axons form appropriate axon arbors in the caudal and superficial part of the SC (***B4***) but also ectopic branches rostrally (***B1***, ***B3***) and in the ventral portion of the mesencephalic slice (***B2***) ($n = 4$ reconstructed axons).

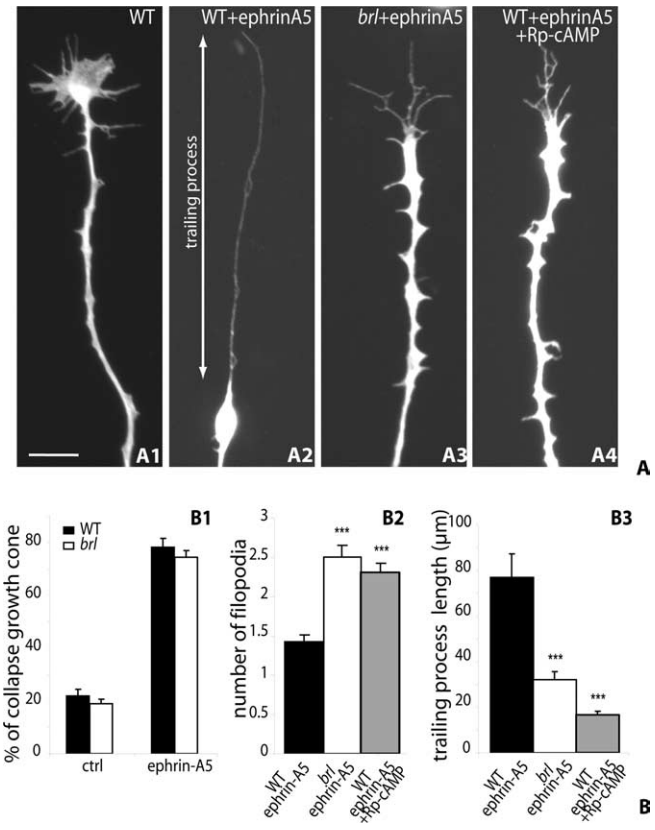

Figure 7. Lack of AC1 modifies the collapse response of retinal growth cones to ephrin-A5. ***A***, A retinal collapse response was induced by ephrin-A5 (250 ng/ml) on E14.5 retinal explants that had grown for 24 h on laminin-coated coverslips. The preparations were fixed 30 min later and immunostained with anti-GFP. ***A1***, WT retinal axon grown in control medium. ***A2***, WT retinal axon 30 min after ephrin-A5 addition. ***A3***, AC1$^{brl/brl}$ retinal axon 30 min after ephrin-A5 application. ***A4***, Retinal axon to which Rp-cAMP (1 μM) was added 30 min before the ephrin-A5 application. The trailing process was measured as the distance between the extremity of the retracting filopodium and the retraction bulb (as indicated in ***A2***). Scale bar, 10 μm. ***B***, Quantification of the collapse responses on preparations fixed 30 min after ephrin-A5 application. ***B1***, The proportion of collapsed growth cones after ephrin-A5 application is similar in AC1$^{brl/brl}$ and WT retinal explants and it is not modified by PKA inhibitors ($n > 200$ per condition; in 3 independent experiments). ***B2***, The morphology of the growth cone was evaluated by counting the number of filopodia that remained attached to the retraction bulb. In control conditions, there is generally only one retracting filopodium; in the AC1$^{brl/brl}$ retinas, two to three filopodia were more frequently observed giving a "forked" appearance as shown in ***A3***. ***$p < 0.001$; unpaired Student's t test. ***B3***, The length of the trailing process measured 30 min after ephrin-A5 application is significantly reduced in axons from AC1$^{brl/brl}$ retinas and after PKA blockade with Rp-cAMP (1 μM) ($n > 80$ axons per condition; 3 independent experiments). Error bars represent SEM.

growth cones. cAMP and protein kinase A (PKA) signaling has not yet been involved in mediating the cellular responses to ephrin As (Shamah et al., 2001; Knoll and Drescher, 2004; Sahin et al., 2005) or of ephrin Bs, although cGMP is implicated in the collapse response of ephrin B1 (Mann et al., 2003). We therefore questioned the implication of cAMP in our collapse assay by acutely administering the PKA inhibitor Rp-cAMP (1 μM), the cyclase inhibitor SQ 22536 [9-(tetrahydro-2′-furyl)adenine] (10 μM), and the cyclase activator forskolin (10 μM) to WT retinal explants. These acute treatments, administered 1 h before the collapse assay, had similar consequences on the collapse response as the loss of function of AC1: the number of remaining filopodia was increased, and the retraction course of the cone was decreased (this is shown for Rp-cAMP in Fig. 7*A4*,*B2*,*B3*).

The observation that both increasing and decreasing cAMP levels in the cones had similar effects on the dynamics of the growth cone suggests that an alteration in the fine spatiotemporal regulation of cAMP is responsible for the changes observed in the AC1$^{brl/brl}$ retinal axons, rather than a global change in cAMP levels. This interpretation is supported by evidence showing that a tight spatial and temporal compartmentalization of cAMP is required for an appropriate cAMP signaling in different physiological contexts (Cooper et al., 1995; Gorbunova and Spitzer, 2002; Zaccolo and Pozzan, 2003).

Discussion

Using a new coculture assay that reproduces the gradual acquisition of topographic specificity of retinal axon targeting, we demonstrate that AC1 is required in the retina for the establishment of regionally selective axon terminal arbors in the SC. We show that these alterations are partly linked to a defective readout of inhibitory positional cues in the SC.

A new model to study retinotectal topographic mapping and collateral elimination

Compared with previous *in vitro* models developed to analyze the mechanisms of retinotectal map formation (Walter et al., 1987;

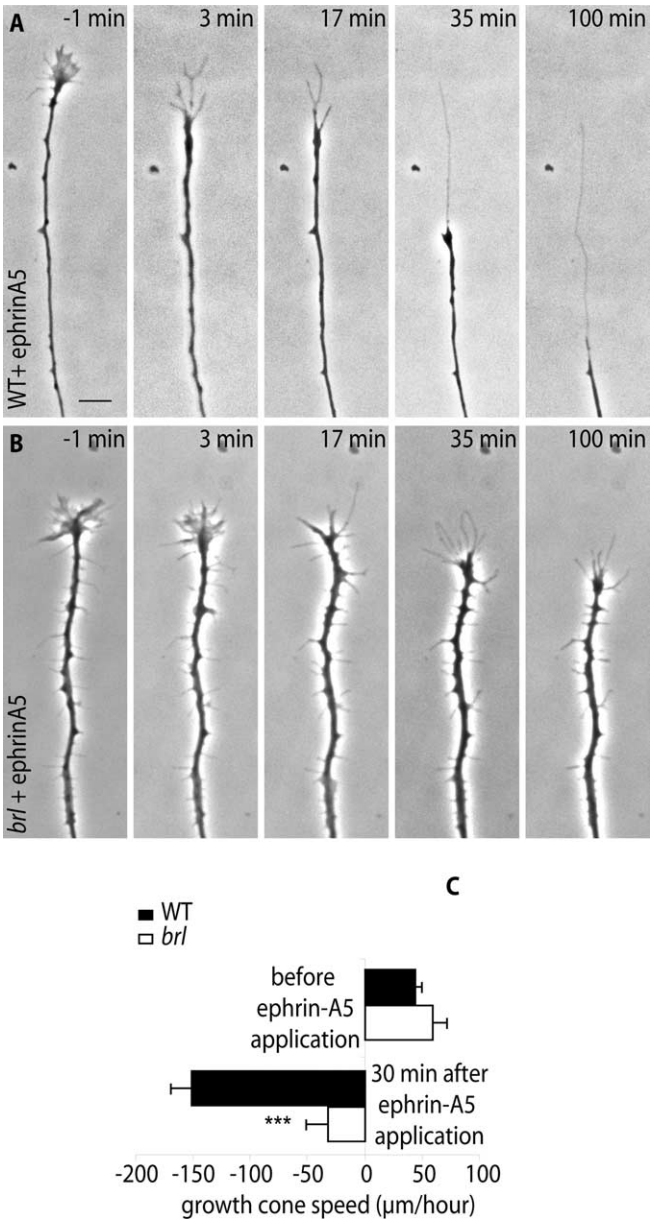

Figure 8. Lack of AC1 arrests the rearward movement of the growth cone induced by ephrin-A5. ***A***, Sequence of a growth cone collapse response induced by ephrin-A5 (time, 0 min) in WT and mutants. In both cases, the axons stopped growing and the lamellipodia disappeared from the growth cone. However, the AC1$^{brl/brl}$ retinal axon fails to effect a rearward movement, at 35 or 100 min after ephrin-A5 application. Scale bar, 10 μm. ***B***, The velocity of the retinal growth cone advance (positive values) or retraction (negative values) was measured 1 h before and 30 min after the application of ephrin-A5. WT, $n = 7$; AC1$^{brl/brl}$, $n = 9$. ***$p < 0.001$ (Student's t test). Error bars represent SEM.

Davenport et al., 1999; Wahl et al., 2000), the interest of the present model is that it recapitulates the late remodeling of the axon arbors as they reach their terminal targets. Interestingly, the *in vitro* timing of events matches the *in vivo* tempo of maturation of the retinal axons. The axon exuberance of retinal axons at 4 DIV corresponds to the *in vivo* overgrowth of retinal axons in the SC at P1; the formation of axon branches at 8 DIV and their increased complexity at 12 DIV matches the elaboration of axon collateral branches during the first postnatal week (Sachs et al., 1986; Simon and O'Leary, 1992).

The retinal axonal reorganizations observed in the organotypic coculture preparation reproduce two developmental processes: (1) the acquisition of a laminar selectivity and (2) the acquisition of a topographic selectivity.

The acquisition of a target specificity is reflected by the ventral to dorsal reorganization of the retinal axons in the slice. This reorganization is linked to the experimental situation in which the RGCs reach the SC by abnormal ventral routes instead of reaching it from the optic tract dorsally. The growth of the RGCs within the entire explant, including in nontarget areas, probably reflects the initial insensitivity of embryonic RGCs to repulsive cues present in nontarget areas. The growth potential of embryonic retinal axons was observed previously in a retinotectal preparation (Chen et al., 1995). Embryonic retinal cells grow on inhibitory substrates (Hankin and Lund, 1987; Cai et al., 2001). The secondary reorientation of the retinal axons toward the optic layers of the SC indicates that the retinal axons keep growing until they have encountered their proper terminal zone and are able to reorient their trajectories, as *in vivo* (Hankin and Lund, 1987; Holt and Harris, 1998). Comparable observations of appropriate laminar targeting were also made in other organotypic coculture systems, such as the thalamocortical preparation (Bolz et al., 1990; Molnar and Blakemore, 1999) or hippocampal organotypic cultures (Zimmer and Gahwiler, 1987; Mizuhashi et al., 2001). However, the description of a transient phase of axonal exuberance is an original contribution of the present model, as is the observation that the axons establish a topographic projection.

Presynaptic role of AC1 for axon remodeling

The AC1$^{brl/brl}$ mice were first characterized by their lack of cortical barrels (Welker et al., 1996; Abdel-Majid et al., 1998) and then shown to display an altered formation of the retinotectal and retinogeniculate maps (Ravary et al., 2003). A presynaptic role of AC1 was proposed because AC1 is negatively coupled to the presynaptic 5-HT$_{1B}$ receptor, the excessive activation of which induces alterations that are very similar to those of the AC1$^{brl/brl}$ (Erzurumlu and Kind, 2001; Gaspar et al., 2003). Moreover, in the developing retinotectal system, AC1 is strongly expressed in the RGCs and only mildly in the SC (Ravary et al., 2003; Nicol et al., 2005). However, because AC1 is necessary for postsynaptic plasticity in the somatosensory cortex (Lu et al., 2003), similar mechanisms were suggested to occur in the retinotectal system (Plas et al., 2004). The present experiments unambiguously demonstrate that AC1 is required in the retina and not in the SC, during the first stages of axon terminal remodeling.

AC1 is one of the nine transmembrane AC isoforms that produce cAMP in response to extrinsic signals. As all cyclases, AC1 is activated by Gs-coupled receptors. In addition, and more specifically, AC1 is activated by Ca^{2+} influx through voltage-sensitive Ca^{2+} channels and is negatively coupled to Gi heterotrimeric proteins (Xia and Storm, 1997; Cooper et al., 1998). Total AC activity is unchanged in the AC1$^{brl/brl}$ retinas, indicating that other isoforms in the retina and SC compensate for the lack of AC1 (Ravary et al., 2003). This sustained capacity to produce cAMP explains why, despite the demonstrated role of cAMP signaling for the survival and growth of RGCs (Meyer-Franke et al., 1995) or for early retinal guidance (Hopker et al., 1999; Trousse et al., 2001), no changes in the early development of the retinal projections are observed in the AC1$^{brl/brl}$. Thus, AC1-mediated signaling could be essentially required during the activity-dependent remodeling of the connections. Indeed, the characteristics of AC1 activation by Ca^{2+} entry make it an interesting candidate in the conversion of the spontaneous neural activity and Ca^{2+} waves into cAMP signaling. Such coupling of Ca^{2+} and cAMP transients has been well documented in other cell types

(Cooper et al., 1995; Gorbunova and Spitzer, 2002; Zaccolo and Pozzan, 2003). Because spontaneous Ca^{2+} waves occur in the developing retina (for review, see Wong, 1993), one could hypothesize that AC1 acts by transforming the Ca^{2+} waves in the retina into cAMP transients in the retinal axons.

Our analysis of the $AC1^{brl/brl}$ axon arbors shows that the major alteration is the maintenance of exuberant ectopic branches, whereas the capacity to form complex branches is unaffected. This is consistent with observations in the somatosensory cortex of the $AC1^{brl/brl}$ mice *in vivo*, showing a normal amount and complexity of thalamocortical branches despite an enlargement of the axon terminal fields in layer IV (Welker et al., 1996; Hage, 2003). It is also possible that the axons are unable to respond to stop signals and continue their growth. Dynamic investigations of single axons over long periods will be required to determine how AC1 controls these different cellular processes and contributes to the elaboration of the terminal field.

AC1 is required for the ephrin-A5-induced retraction of retinal axons

Our observations indicate that the effects of AC1 are mediated in part by a modification of the response of retinal growth cones to ephrin-As. Ephrin-As act primarily as repellents of axon growth, causing the axons to stop and collapse (Cheng et al., 1995; Drescher et al., 1995; Wahl et al., 2000). Ephrin-A also induced axon growth and collateral branching (Castellani et al., 1998; Yates et al., 2001). Accordingly, in our coculture assay, the blockade of the ephrin-A signaling prevented the retraction of exuberant temporal retinal axons and alters the branching selectivity of nasal and temporal retinal axons, thereby mimicking the consequences of the lack of AC1 in the retina. However, a difference was observed in the two conditions, because the blockade of ephrin-As, unlike the lack of AC1, reduced axon collateral branching, indicating that some of the effects of ephrin-A signaling are independent of AC1.

A direct interaction between AC1 and the ephrin-As was demonstrated by the observation of a modified ephrin-induced collapse response in the $AC1^{brl/brl}$. The alterations of the response of the $AC1^{brl/brl}$ retinal axons to ephrin-A5 were restricted to a late phase of the collapse: the rearward migration of the cone. Similar observations were made after interfering with cytoskeletal components or Rho-GTPases (Baas and Ahmad, 2001; Thies and Davenport, 2003).

Signaling by ephrin-A5 is mediated by EphA3 and EphA5 receptors in RGCs. It is unlikely that a reduced expression of these receptors occurs in the $AC1^{brl/brl}$ mutants, because the acute administration of AC or PKA inhibitors in WT explants reproduces the abnormalities of the $AC1^{brl/brl}$. Alternatively, there may be a cross-talk between cAMP and Eph receptors. Binding of ephrins to their Eph receptors triggers complex signaling cascades (Shamah et al., 2001; Knoll and Drescher, 2004; Sahin et al., 2005) in which cAMP and PKA could act directly or downstream of the Eph receptor cascade.

The interaction of AC1 and ephrin-A signaling explains a large part of the mapping alterations of the AC1-deficient mice but does not suffice to explain the entirety of the phenotype *in vivo*. The ephrin-A2/A5 DKO and the $AC1^{brl/brl}$ mice display altered retinotopic maps, but the organization of axon terminal arbors differ. In the ephrin-A2/A5 double knock-out (DKO) mice, retinal axons form multiple terminal zones along the rostrocaudal extent of the SC (Feldheim et al., 2000), but axon arbors appear to be limited in extent. One likely explanation is that competitive interactions between the retinal axons, which determine the size of individual axon arbors, continue to occur in the ephrin-A2/A5 DKO (Pfeiffenberger et al., 2005) but not in the $AC1^{brl/brl}$. These later steps may then involve synaptic competition mechanisms that are not appropriately modeled in the culture slice preparation.

In conclusion, our results demonstrate a cell autonomous role of AC1 in the RGCs of the retina for the selection of appropriate terminal targets. It shows that AC1 is needed for the normal retraction response of the retinal axons to ephrin-A5. These data indicate that the abnormal establishment of retinal maps in the $AC1^{brl/brl}$ could result, in large part, from a defective readout of membrane-bound repulsive cues, causing alterations in the large-scale remodeling of the axons.

References

Abdel-Majid RM, Leong WL, Schalkwyk LC, Smallman DS, Wong ST, Storm DR, Fine A, Dobson MJ, Guernsey DL, Neumann PE (1998) Loss of adenylyl cyclase I activity disrupts patterning of mouse somatosensory cortex. Nat Genet 19:289–291.

Baas PW, Ahmad FJ (2001) Force generation by cytoskeletal motor proteins as a regulator of axonal elongation and retraction. Trends Cell Biol 11:244–249.

Bolz J, Novak N, Gotz M, Bonhoeffer T (1990) Formation of target-specific neuronal projections in organotypic slice cultures from rat visual cortex. Nature 346:359–362.

Cai D, Qiu J, Cao Z, McAtee M, Bregman BS, Filbin MT (2001) Neuronal cyclic AMP controls the developmental loss in ability of axons to regenerate. J Neurosci 21:4731–4739.

Castellani V, Yue Y, Gao PP, Zhou R, Bolz J (1998) Dual action of a ligand for Eph receptor tyrosine kinases on specific populations of axons during the development of cortical circuits. J Neurosci 18:4663–4672.

Chen DF, Jhaveri S, Schneider GE (1995) Intrinsic changes in developing retinal neurons result in regenerative failure of their axons. Proc Natl Acad Sci USA 92:7287–7291.

Cheng HJ, Nakamoto M, Bergemann AD, Flanagan JG (1995) Complementary gradients in expression and binding of elf-1 nad mek4 in development of the topographic retinotectal projection map. Cell 82:371–381.

Ciossek T, Monschau B, Kremoser C, Loschinger J, Lang S, Muller BK, Bonhoeffer F, Drescher U (1998) Eph receptor-ligand interactions are necessary for guidance of retinal ganglion cell axons in vitro. Eur J Neurosci 10:1574–1580.

Cline H (2003) Sperry and Hebb: oil and vinegar? Trends Neurosci 26:655–661.

Cooper DM, Mons N, Karpen JW (1995) Adenylyl cyclases and the interaction between calcium and cAMP signalling. Nature 374:421–424.

Cooper DM, Schell MJ, Thorn P, Irvine RF (1998) Regulation of adenylyl cyclase by membrane potential. J Biol Chem 273:27703–27707.

Davenport RW, Thies E, Cohen ML (1999) Neuronal growth cone collapse triggers lateral extensions along trailing axons. Nat Neurosci 2:254–259.

Drescher U, Kremoser C, Handwerker C, Loschinger J, Noda M, Bonhoeffer F (1995) In vitro guidance of retinal ganglion cell axons by RAGS, a 25 kDa tectal protein related to ligands for Eph receptor tyrosine kinases. Cell 82:359–370.

Erzurumlu RS, Kind PC (2001) Neural activity: sculptor of "barrels" in the neocortex. Trends Neurosci 24:589–595.

Feldheim DA, Kim YI, Bergemann AD, Frisen J, Barbacid M, Flanagan JG (2000) Genetic analysis of ephrin-A2 and ephrin-A5 shows their requirement in multiple aspects of retinocollicular mapping. Neuron 25:563–574.

Frisen J, Yates PA, McLaughlin T, Friedman GC, O'Leary DD, Barbacid M (1998) Ephrin-A5 (AL-1/RAGS) is essential for proper retinal axon guidance and topographic mapping in the mammalian visual system. Neuron 20:235–243.

Gaspar P, Cases O, Maroteaux L (2003) The developmental role of serotonin: news from mouse molecular genetics. Nat Rev Neurosci 4:1002–1012.

Goodhill GJ, Richards LJ (1999) Retinotectal maps: molecules, models and misplaced data. Trends Neurosci 22:529–534.

Gorbunova YV, Spitzer NC (2002) Dynamic interactions of cyclic AMP transients and spontaneous Ca(2+) spikes. Nature 418:93–96.

Hadjantonakis AK, Gertsenstein M, Ikawa M, Okabe M, Nagy A (1998) Generating green fluorescent mice by germline transmission of green fluorescent ES cells. Mech Dev 76:79–90.

Hage I (2003) Early postnatal development of thalamocortical axons to barrel cortex in NOR and barrelless mice a morphological tracing study. PhD thesis, Université de Lausanne.

Hankin MH, Lund RD (1987) Specific target-directed axonal outgrowth from transplanted embryonic rodent retinae into neonatal rat superior colliculus. Brain Res 408:344–348.

Holt CE, Harris WA (1998) Target selection: invasion, mapping and cell choice. Curr Opin Neurobiol 8:98–105.

Hopker VH, Shewan D, Tessier-Lavigne M, Poo M, Holt C (1999) Growth-cone attraction to netrin-1 is converted to repulsion by laminin-1. Nature 401:69–73.

Knoll B, Drescher U (2002) Ephrin-As as receptors in topographic projections. Trends Neurosci 25:145–149.

Knoll B, Drescher U (2004) Src family kinases are involved in EphA receptor-mediated retinal axon guidance. J Neurosci 24:6248–6257.

Lohof AM, Quillan M, Dan Y, Poo MM (1992) Asymmetric modulation of cytosolic cAMP activity induces growth cone turning. J Neurosci 12:1253–1261.

Lu HC, She WC, Plas DT, Neumann PE, Janz R, Crair MC (2003) Adenylyl cyclase I regulates AMPA receptor trafficking during mouse cortical "barrel" map development. Nat Neurosci 6:939–947.

Lund RD, Lund JS (1972) Development of synaptic patterns in the superior colliculus of the rat. Brain Res 42:1–20.

Luo L, O'Leary DD (2005) Axon retraction and degeneration in development and disease. Annu Rev Neurosci 28:127–156.

Mann F, Miranda E, Weinl C, Harmer E, Holt CE (2003) B-type Eph receptors and ephrins induce growth cone collapse through distinct intracellular pathways. J Neurobiol 57:323–336.

Mattson MP, Taylor-Hunter A, Kater SB (1988) Neurite outgrowth in individual neurons of a neuronal population is differentially regulated by calcium and cyclic AMP. J Neurosci 8:1704–1711.

McLaughlin T, Hindges R, O'Leary DD (2003a) Regulation of axial patterning of the retina and its topographic mapping in the brain. Curr Opin Neurobiol 13:57–69.

McLaughlin T, Torborg CL, Feller MB, O'Leary DD (2003b) Retinotopic map refinement requires spontaneous retinal waves during a brief critical period of development. Neuron 40:1147–1160.

Meyer-Franke A, Kaplan MR, Pfrieger FW, Barres BA (1995) Characterization of the signaling interactions that promote the survival and growth of developing retinal ganglion cells in culture. Neuron 15:805–819.

Mizuhashi S, Nishiyama N, Matsuki N, Ikegaya Y (2001) Cyclic nucleotide-mediated regulation of hippocampal mossy fiber development: a target-specific guidance. J Neurosci 21:6181–6194.

Molnar Z, Blakemore C (1999) Development of signals influencing the growth and termination of thalamocortical axons in organotypic culture. Exp Neurol 156:363–393.

Nicol X, Muzerelle A, Bachy I, Ravary A, Gaspar P (2005) Spatiotemporal localisation of the calcium stimulated cyclase, AC1 and AC8, during mouse brain development. J Comp Neurol 486:281–294.

Pfeiffenberger C, Cutforth T, Woods G, Yamada J, Renteria RC, Copenhagen DR, Flanagan JG, Feldheim DA (2005) Ephrin-As and neural activity are required for eye-specific patterning during retinogeniculate mapping. Nat Neurosci 8:1022–1027.

Plas DT, Visel A, Gonzalez E, She WC, Crair MC (2004) Adenylate Cyclase 1 dependent refinement of retinotopic maps in the mouse. Vision Res 44:3357–3364.

Ravary A, Muzerelle A, Herve D, Pascoli V, Ba-Charvet KN, Girault JA, Welker E, Gaspar P (2003) Adenylate cyclase 1 as a key actor in the refinement of retinal projection maps. J Neurosci 23:2228–2238.

Rodger J, Lindsey KA, Leaver SG, King CE, Dunlop SA, Beazley LD (2001) Expression of ephrin-A2 in the superior colliculus and EphA5 in the retina following optic nerve section in adult rat. Eur J Neurosci 14:1929–1936.

Sachs GM, Jacobson M, Caviness Jr VS (1986) Postnatal changes in arborization patterns of murine retinocollicular axons. J Comp Neurol 246:395–408.

Sahin M, Greer PL, Lin MZ, Poucher H, Eberhart J, Schmidt S, Wright TM, Shamah SM, O'Connell S, Cowan CW, Hu L, Goldberg JL, Debant A, Corfas G, Krull CE, Greenberg ME (2005) Eph-dependent tyrosine phosphorylation of ephexin1 modulates growth cone collapse. Neuron 46:191–204.

Shamah SM, Lin MZ, Goldberg JL, Estrach S, Sahin M, Hu L, Bazalakova M, Neve RL, Corfas G, Debant A, Greenberg ME (2001) EphA receptors regulate growth cone dynamics through the novel guanine nucleotide exchange factor ephexin. Cell 105:233–244.

Simon DK, O'Leary DD (1992) Development of topographic order in the mammalian retinocollicular projection. J Neurosci 12:1212–1232.

Song H, Ming G, He Z, Lehmann M, McKerracher L, Tessier-Lavigne M, Poo M (1998) Conversion of neuronal growth cone responses from repulsion to attraction by cyclic nucleotides. Science 281:1515–1518.

Thies E, Davenport RW (2003) Independent roles of Rho-GTPases in growth cone and axonal behavior. J Neurobiol 54:358–369.

Trousse F, Marti E, Gruss P, Torres M, Bovolenta P (2001) Control of retinal ganglion cell axon growth: a new role for Sonic hedgehog. Development 128:3927–3936.

Upton AL, Salichon N, Lebrand C, Ravary A, Blakely R, Seif I, Gaspar P (1999) Excess of serotonin (5-HT) alters the segregation of ispilateral and contralateral retinal projections in monoamine oxidase A knock-out mice: possible role of 5-HT uptake in retinal ganglion cells during development. J Neurosci 19:7007–7024.

Upton AL, Ravary A, Salichon N, Moessner R, Lesch KP, Hen R, Seif I, Gaspar P (2002) Lack of 5-HT-1B receptor and of serotonin transporter have a different effect on the segregation of retinal axons in the lteral geniculate nucleus and the superior colliculus. Neuroscience.

Villacres EC, Wu Z, Hua W, Nielsen MD, Watters JJ, Yan C, Beavo J, Storm DR (1995) Developmentally expressed Ca(2+)-sensitive adenylyl cyclase activity is disrupted in the brains of type I adenylyl cyclase mutant mice. J Biol Chem 270:14352–14357.

Wahl S, Barth H, Ciossek T, Aktories K, Mueller BK (2000) Ephrin-A5 induces collapse of growth cones by activating Rho and Rho kinase. J Cell Biol 149:263–270.

Walter J, Kern-Veits B, Huf J, Stolze B, Bonhoeffer F (1987) Recognition of position-specific properties of tectal cell membranes by retinal axons in vitro. Development 101:685–696.

Welker E, Armstrong-James M, Bronchti G, Ourednik W, Gheorghita-Baechler F, Dubois R, Guernsey DL, Van der Loos LH, Neumann PE (1996) Altered sensory processing in the somatosensory cortex of the mouse mutant barrelless. Science 271:1864–1867.

Wong RO (1993) The role of spatio-temporal firing patterns in neuronal development of sensory systems. Curr Opin Neurobiol 3:595–601.

Xia Z, Storm DR (1997) Calmodulin-regulated adenylyl cyclases and neuromodulation. Curr Opin Neurobiol 7:391–396.

Yates PA, Roskies AL, McLaughlin T, O'Leary DD (2001) Topographic-specific axon branching controlled by ephrin-As is the critical event in retinotectal map development. J Neurosci 21:8548–8563.

Zaccolo M, Pozzan T (2003) cAMP and Ca^{2+} interplay: a matter of oscillation patterns. Trends Neurosci 26:53–55.

Zimmer J, Gahwiler BH (1987) Growth of hippocampal mossy fibers: a lesion and coculture study of organotypic slice cultures. J Comp Neurol 264:1–13.